



# Coral skeletons reveal the impacts of oil pollution on seawater chemistry in the northern South China Sea

Sirong Xie<sup>a,c</sup>, Wei Jiang<sup>a,b,\*</sup>, Chunmei Feng<sup>a</sup>, Yinan Sun<sup>a</sup>, Yansong Han<sup>a</sup>, Yuwen Xiao<sup>a</sup>, Chaoshuai Wei<sup>a</sup>, Kefu Yu<sup>a,b,\*\*</sup>

<sup>a</sup> Guangxi Laboratory on the Study of Coral Reefs in the South China Sea, School of Marine Sciences, Guangxi University, Nanning, 530004, China

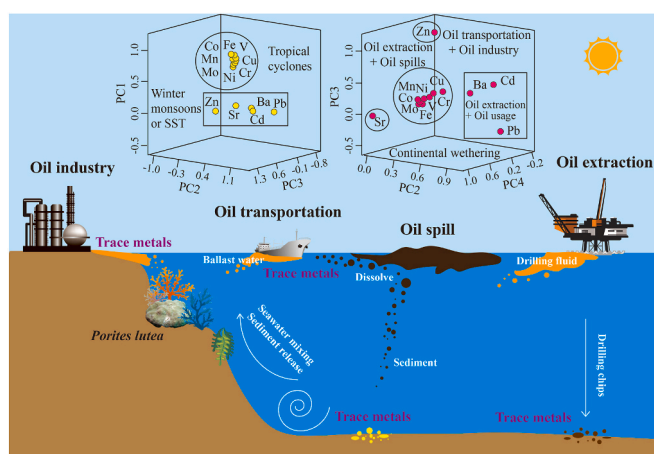
<sup>b</sup> Southern Marine Science and Engineering Guangdong Laboratory (Zhuhai), Zhuhai, 519080, China

<sup>c</sup> School of Resources, Environment and Materials, Guangxi University, Nanning, 530004, China

## HIGHLIGHTS

- High-resolution coral skeletons can be used as a novel tool for marine pollution.
- Contribution of oil pollution to each trace metal in surface seawater was estimated.
- Effects of oil spills on trace metal in surface seawater can last for ~1.4 months.

## GRAPHICAL ABSTRACT



## ARTICLE INFO

Handling Editor: Milena Horvat

### Keywords:

*Porites lutea*  
Oil spill  
Trace metals  
Weizhou island

## ABSTRACT

Oil pollution can release trace metals (TMs) with cumulative toxicity into seawater, harming marine ecosystems in the long term. However, the lack of studies has inhibited our understanding of the effects and mechanisms of oil pollution on TMs in seawater. Hence, we investigated the 10-year monthly variation of TMs in *Porites* coral skeletons from the northern South China Sea (SCS), complemented by spatial distribution of TMs in seawater, sediments and characterization of TMs in fuel oil. The results of principal component-multivariate linear regression showed that the total contribution of oil pollution as a source to TMs in surface seawater was 77.2%, where the residence time of TMs (Ni, V, Cr, Co, Cu, Mn, Fe, and Mo) released from oil spills in surface seawater was approximately 1.4 months. Due to the geochemical nature of the metals, their seasonal variations are

\* Corresponding author. Guangxi Laboratory on the Study of Coral Reefs in the South China Sea; School of Marine Sciences, Guangxi University, Nanning, 530004, China.

\*\* Corresponding author. Guangxi Laboratory on the Study of Coral Reefs in the South China Sea, School of Marine Sciences, Guangxi University, Nanning, 530004, China.

E-mail addresses: [jianwe@gxu.edu.cn](mailto:jianwe@gxu.edu.cn) (W. Jiang), [kefuyu@socio.ac.cn](mailto:kefuyu@socio.ac.cn) (K. Yu).

<https://doi.org/10.1016/j.chemosphere.2023.139632>

Received 10 April 2023; Received in revised form 20 July 2023; Accepted 22 July 2023

Available online 22 July 2023

0045-6535/© 2023 Elsevier Ltd. All rights reserved.

controlled by tropical cyclones (Ni, V, Cr, Co, Cu, Mn, Fe, and Mo), winter monsoons (Pb, Cd, Ba, and Zn) and sea surface temperature (Sr). This study shows that coral skeletons can be used as a new tool to study marine oil pollution. This provides valuable reference data for accurately identifying and quantifying the effects of oil pollution on TMs in seawater from a spatial and temporal perspective.

## 1. Introduction

Oil is considered the main power energy source of modern industrial society and often referred to as the “blood” of the industry (Chen et al., 2019; Zhu et al., 2013). However, the increased demand for oil has led to an increase in oil pollution caused by oil and its refinery products (gasoline, kerosene, diesel, etc.) entering the marine environment during extraction, transportation, refining, storage, and use. This is particularly true with oil spills at sea (Dong et al., 2022a; Gong et al., 2020). Once oil enters the ocean, it undergoes various processes such as evaporation, dissolution, dispersion, photo-oxidative degradation, emulsification, biodegradation, adsorption, sedimentation (Passow and Overton, 2021), which result in the release of hydrocarbons and trace metals (TMs) into the seawater (Li et al., 2020). While hydrocarbons can be readily degraded by photo-oxidation, TMs are persistent and have cumulative toxicity, which means they can cause long-term damage to marine ecosystems (King et al., 2014). Several studies have shown that oil pollution (oil spills, marine oil extraction, coastal oil industry, oil terminals, tanker transportation) can cause abnormal increases in TMs contents in the seawater and sediments (Breuer et al., 2004; Bu-Olayan et al., 1998; Duleba et al., 2019; Wang et al., 2019), making TMs, especially V and Ni, useful indicators to identify oil pollution events (Gong et al., 2020; Guzman and Jarvis, 1996; Li et al., 2020; Wu et al., 2022). However, the effects of marine oil pollution on surface seawater may only last a few weeks to a few months (Vaz et al., 2021), and most of the TMs released into the water phase settle and adsorb into the sediments (Liu et al., 2012). In addition, traditional methods for assessing seawater TMs (e.g., surface seawater, surface sediments) tend to focus on spatial characteristics (Tao et al., 2021), making it difficult to explore oil pollution on seawater TMs in time series, while sediment cores usually have low resolution (Amorosi, 2012), limiting our ability to understand the effect of oil pollution on seawater TMs in terms of spatial characteristics and temporal dynamics and to determine the contribution of each metal (Ahmad et al., 2015).

*Porites* corals are sensitive to environmental changes and have large annual growth, clear interannual boundaries, long continuous growth, good system closure, rich information content, wide distribution, and aragonitic skeletons suitable for dating (Kinzie and Buddemeier, 1996), making them excellent materials for recording annual, seasonal and monthly high-resolution environmental changes in the ocean. Trace elements can be incorporated into coral's aragonite lattice in proportion to their concentrations in ambient seawater (Chen et al., 2015). Therefore, variations in the concentration of trace elements in coral skeletons mainly indicate changes in seawater. Indeed, high-resolution geochemical records of *Porites* coral skeletal TMs on long-time scales have proven to be powerful indicator tools for the long-term monitoring of changes in the marine environment (Saha et al., 2016). For example, researchers have used the records of TMs in *Porites* coral skeletons to reveal environmental changes associated with anthropogenic activities, such as coastal projects (Prouty et al., 2008; Nguyen et al., 2013), industrial emissions (Shen and Boyle, 1987), ship pollution (Song et al., 2014; Inoue et al., 2004), and oil pollution (Guzman and Jarvis, 1996; Wu et al., 2022). Furthermore, natural factors such as terrestrial input (Chen et al., 2015; Lewis et al., 2018), ocean and atmospheric disturbances (Shen et al., 1992; Jiang et al., 2017; Wu et al., 2022), and biological effects (Spooner et al., 2018; Neira et al., 2022) can dominate the variability of TMs in coral skeletons in the absence of specific anthropogenic influences. Thus, reef-building corals are reliable biomonitors of marine TMs pollution and contribute to our understanding

of the sources, geochemical behavior, and environmental significance of TMs in seawater.

Weizhou Island (WZI) in the northern South China Sea (SCS) distributes a complex array of marine oil extraction and oil industries where oil spills have occurred. Previous work on the impacts of oil pollution on WZI and the northern SCS as a whole has tended to focus on direct impacts on hydrocarbons (Yu et al., 2019; Zhang et al., 2021). The quantitative and temporal variability of TMs released from marine oil pollution has not been assessed due to the lack of continuous monitoring systems. However, monitoring techniques based on the elemental content of coral skeletons can be used to address this issue. In addition, previous time series using TMs from coral skeletons to record marine geochemical changes (Jiang et al., 2017; Song et al., 2014) were limited to annual resolution, which had difficulty capturing events like marine oil pollution that affect surface waters for only a few weeks to a few months, and no relevant studies of monthly resolution have yet emerged.

In this study, we collected *Porites* corals, seawater, sediments, and fuel oil around WZI in the northern SCS and investigated the temporal variation of lattice-like TMs in coral skeletons at monthly resolution during 2005–2015 AD. Meanwhile, the spatial distribution of TMs in seawater and sediments, and TMs content in fuel oil was explored. The main objective of this study is to accurately assess the varying impact of oil pollution on TMs in seawater by combining spatial features and high-resolution time series while quantifying the contribution of oil pollution to each TM present in surface seawater. This provides valuable data for understanding the dynamic effects of oil pollution on TMs in seawater from both spatial and temporal perspectives.

## 2. Materials and methods

### 2.1. Study site and coral sampling

WZI is located in the Beibu Gulf, northern SCS, and is an island built up by volcanic eruptions and surrounded by coral reefs, belonging to the high-latitude coral reef area, with prevailing East Asian tropical monsoon. The collection location of *Porites lutea* coral labeled as W3 (21°47'N, 109°5'24"E) is shown in Fig. 1, and the sampling depth is 4 m. Coral species were identified using their apparent morphology and their skeletal structure, with reference to Corals of the World (Veron, 2000). In October 2015, one coral core was collected and washed with water to remove surface impurities. Coral core was cut into ~8 mm thick slice along the main growth axis. The coral slice was soaked in 10% H<sub>2</sub>O<sub>2</sub> for 48 h and cleaned three times with Mill-Q water in an ultrasonic bath to ensure that remove any surface contamination that could influence trace elemental records. Our previous study established the chronological frame of the W3 *Porites lutea* coral skeleton using high-resolution  $\delta^{18}\text{O}$ , sea surface temperature (SST), and X-radiography positive print (Xu et al., 2018). The annual column within the coral skeleton consists of high (dark) and low (bright) density cycles. Whereas the coral skeleton  $\delta^{18}\text{O}$  is negatively correlated with SST, with one cycle change representing 1 year (Figure S1 in the supplementary materials), the chronological framework is cross-validated by  $\delta^{18}\text{O}$  and SST. With reference to the time series framework established by X-radiography positive,  $\delta^{18}\text{O}$  and SST, 114 monthly-resolution subsamples were intensively carved and abraded in ~2 mm intervals using a stainless steel blade, with sampling continuously along the coral maximum growth axis during sampling to avoid any seasonal features during the analysis of annual subsamples. Additionally, surface seawater, sediments, and fuel oil

samples from sunken cargo ships were collected around WZI in June 2022 (Fig. 1), with samples collected in triplicate at each site. The collected seawater was filtered through a 0.45  $\mu\text{m}$  filter membrane, and  $\text{HNO}_3$  was added to adjust  $\text{pH} < 2$ .

## 2.2. Geochemical analysis

Preparation of superpure  $\text{HNO}_3$  from GR superior pure  $\text{HNO}_3$  by three subazeotropic distillation. Before configuring the solution to be tested on the machine, the polyethylene bottles were subjected to a rigorous acid-washing procedure, and Mill-Q water and ultrapure  $\text{HNO}_3$  were used to prepare 2%  $\text{HNO}_3$  for use in the experiments. 5 vials of multi-element ICP mixed standard solutions were used to configure standard solutions containing over 50 elements to create the standard curves. Then, W3 coral, seawater, sediments and fuel oil samples were tested. To correct for the matrix effect of instrument drift, 100 mL of 100 ppb internal standard stock solution was prepared with internal standard elements ( $^{103}\text{Rh}$ ,  $^{115}\text{In}$ ,  $^{187}\text{Re}$ ). Geochemical standards (GBW07129, GBW07133 and GBW07135) were used as external standards for coral skeleton analysis, and 1 mL of 100 ppb internal standard stock solution was added and diluted  $\sim 2000$  times with 2%  $\text{HNO}_3$ . Weighed  $\sim 3$  mg of coral skeleton powder was placed in a centrifuge tube, 900  $\mu\text{L}$  of 100 ppb internal standard stock solution was added, the sample was fixed to 18 g with 2%  $\text{HNO}_3$ , and the sample was diluted  $\sim 6000$  times. The seawater standard reference substance NASS-6 (National Research Council Canada, Ottawa Canada) is used as the external standard for seawater analysis. The method reported by Zhang et al. (2023) was used to determine the content of TMs in seawater. The feasibility of similar methods has also been verified by Wei et al. (2013). The seawater samples were diluted 10 times with 2%  $\text{HNO}_3$  containing 6 ppb internal standard stock solution to reduce the salinity to 3‰. In order to further eliminate the matrix effect of salinity and obtain stable test results, the peristaltic pump speed was reduced to 10 rpm, the injection volume per unit time was reduced, the high sensitivity mode was opened, and the voltage of the electronic lens was increased. The residence time of each element was set to 10000 ms, the function of the collision reaction pool was opened, and He was selected as the collision gas with a gas flow rate of 20 mL/min by using the automatic optimization function of the system. The results of TMs in seawater determined in this study are within the range of previous studies around WZI (Table S1 and Table S2). The marine sediment standard reference substance GBW07333 was used as the external standard for sediment analysis. The sediments were dried, milled and sieved (0.15 mm), then weighed 0.1 g in a Teflon digestion tank, 6 mL of aqua regia was added, and digested on an electric hot plate. 0.1 g of fuel oil sample was weighed in a Teflon digestion tank, added 6 mL  $\text{HNO}_3$  and 2 mL  $\text{H}_2\text{O}_2$ ,

and digested on an electric hot plate. The internal standard content in all the solutions to be measured on the machine (sample solution, blank sample, parallel sample, geochemical standard solution, standard solution) was 6 ppb.

Determination of Ni, V, etc. in seawater, sediments, and fuel oil by Inductively Coupled Plasma Mass Spectrometer (ICP-MS). W3 coral skeletal pretreatment sample solutions were tested to determine the concentrations of Ni, V, Pb, Cr, Co, Zn, Cu, Cd, Mn, Fe, Ba, Sr, and Mo using ICP-MS. Standard solutions were measured preferentially to establish a standard curve for quantification, and external standard solutions were subsequently measured to verify the accuracy of the instrument data. Quality assurance and quality control (QA/QC) procedures that included reagent blanks, duplicate tests, and certified geochemical reference materials were applied to assess the accuracy and precision of the analytical data. The national geochemical reference substances (GBW07129, GBW07133, GBW07135, and GBW07333) and seawater standard reference substance (NASS-6) were used for inspection. The relative standard deviations (RSDs) of the results were generally less than 5%, and the recovery rate of internal standard was 85%–115% for all samples measured three times in duplicate. These measurements were accomplished at the Guangxi laboratory on the Study of Coral Reefs in the South China Sea, Guangxi University.

## 2.3. Statistical analysis and graphing

The monthly resolution data were obtained by linear interpolation from the coral chronology. Pearson correlation analysis, principal component analysis (PCA), and multiple linear regression analysis were conducted in this study. Spearman-Rho correlation analysis was performed for TMs in different media (Ortiz-Ojeda and Rázuri-Esteves, 2021). Prior to PCA, the Kolmogorov-Smirnov test was used to assess the distribution status of the dataset. When the distribution was not normal, the data were log-transformed before statistical analysis. The Kaiser-Meyer-Olkin (KMO) value for the PCA is 0.77, indicating that it is interpretable. Interpolated principal component scores were compared with meteorological data and historical event times. Performed data analysis and create graphs using Microsoft Office Excel 2019, IBM SPSS Statistics 26, Origin 2021, and ArcGIS 10.3.

## 3. Results

TMs in seawater, sediments, and fuel oil are shown in Table S3, S4, and Figure S2. The TMs contents in seawater, sediments, and fuel oil were respectively ranked as  $\text{Zn} > \text{Mn} > \text{Cu} > \text{Ni} > \text{Mo} > \text{Pb} > \text{Cr} > \text{Co}$ ,  $\text{Zn} > \text{Ni} > \text{Cr} > \text{Pb} > \text{V} > \text{Co} > \text{Cu} > \text{Mn}$ , and  $\text{Mn} > \text{Zn} > \text{Ni} > \text{Cr} > \text{V} > \text{Cu} > \text{Mo} > \text{Pb} > \text{Co}$ . Compared to Xisha waters without significant

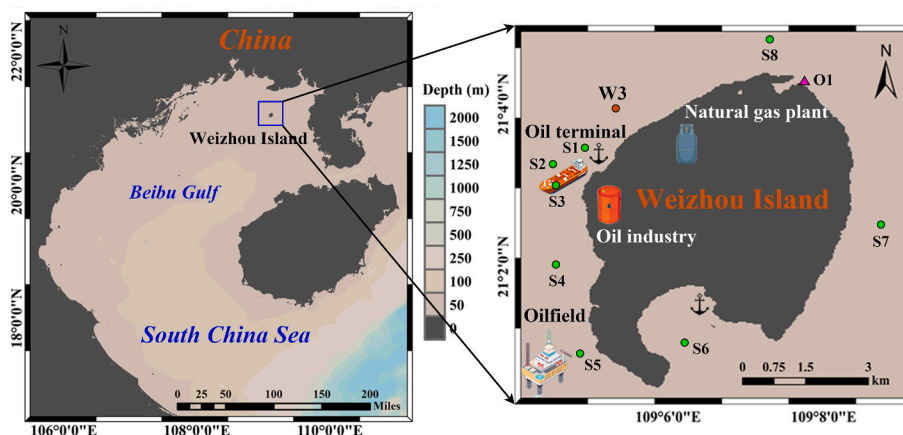


Fig. 1. Location of *Porites* coral sample around WZI, Beibu Gulf, northern South China Sea (The yellow circle is coral sampling site, the green circles are seawater and sediment sampling sites, the pink triangle is fuel oil sampling site).

anthropogenic pollution (Dong et al., 2022b; Li et al., 2022), the seawater and sediments of WZI had higher contents of Cr, Mn, Ni, Cu, Zn, and Pb (Fig. S3). The levels of Cu and Pb in seawater and sediments were also higher in this study than previous studies by WZI (Yang et al., 2017; Liang et al., 2021). Moreover, the levels of Cr, Ni, Zn and Pb in the sediments are higher than in the Suez Bay, while Cr is lower than in the Al-Khobar area (Nour et al., 2022; Alharbi et al., 2022). The contents and temporal variation of TMs in the W3 coral samples were shown in Table 1 and Fig. S4, respectively. The distribution of percentile content and variation of the time-series indicate that all TMs in the W3 coral samples, except Sr, showed skewed distributions, indicating that these TMs fluctuated dramatically over a certain period (2008–2015 AD) and showed abnormally high values. The coefficients of variation (CVs) for Ni, V, Pb, Cr, Co, Zn, Cu, Cd, Mn, Fe, and Mo were very high ( $\geq 90\%$ ) compared to Ba and Sr, indicating a skewed distribution of these TMs in coral skeletons with a very large degree of dispersion, which is caused by high levels of outliers.

Because of the large differences in distribution coefficients of TMs between coral skeletons of different species and seawater (Jiang et al., 2020), we obtained data on TMs in *Porites* coral skeletons from other oil-contaminated seas around the world (Persian Gulf, Red Sea, Central America) to compare with the W3 *Porites* coral skeletons for TMs contamination levels (Table 2). TMs in *Porites* coral skeletons from WZI show a different pattern compared to studies conducted in other oil-active seas. The Ni content of coral skeletons from W3 *Porites* is relatively low, much less than in the oil-active Persian Gulf (Bolouki Kourandeh et al., 2021) and in the Red Sea off Egypt (El-Sorogy et al., 2012; Nour and Nough, 2020), and only higher than the Saudi Arabian coast of the Red Sea (Hanna and Muir, 1990). Cu is also only greater than the Red Sea Saudi Arabia sample. The mean values of V, Cr, and Cd are only higher than in the Persian Gulf. The levels of Pb are greater than in the Persian Gulf and Venezuela of Central America (Bastidas and Garcia, 1999) and much smaller than in the Red Sea. Co is comparable to *Porites* corals from the Persian Gulf and smaller than samples from Egypt in the Red Sea. The levels of Zn are the same as those reported by Al-Rousan et al. (2007) for the Gulf of Aqaba, Jordan. Mn in W3 *Porites* corals may be in a lightly polluted state, comparable only to Hurghada in the Red Sea in Egypt and greater than the Persian Gulf, the Red Sea in Saudi Arabia, the Caribbean Sea, and the Gulf of Aqaba in Jordan. However, the levels of Fe are much higher than in other waters with high oil activity, suggesting that Fe in the coral skeletons of W3 *Porites* may be at moderate contamination levels.

## 4. Discussion

### 4.1. Spatial distribution characteristics of TMs in seawater and sediments

In recent years, with the strong influence of man-made activities such as oil industry, shipping, tourism and oil extraction around WZI, the seawater of WZI is mildly polluted, in which, some TMs content has exceeded the pollution standard many times (Xu et al., 2018; Yang et al., 2017). To explore the spatial distribution characteristics of TMs, kriging

interpolation was performed on TMs contents in seawater and sediments. Fig. 2 shows that there is clear spatial heterogeneity in the distribution of TMs in seawater, with Cr, Mn, Co, Ni, Cu, Zn, Mo, and Pb showing a spatial trend of high in the west and low in the east. It is noteworthy that the highest contents of all these metals occur in the northwest, where oil spills are prone to occur near ship lanes, oil terminals, and oil industries. Among them, Mn, Ni, Mo, Pb, and Co show identical content order in seawater as in fuel oil (Table S3 and Figure S2). Furthermore, the analysis of sediments as an important source and sink of trace elements in seawater is necessary. As shown in Fig. 3, TMs in sediments also exhibit a similar spatial heterogeneity to seawater, with high contents of V, Cr, Mn, Co, Ni, Cu, Zn, and Pb also showing a spatial trend of high in the west, where several serious oil spills had occurred and low in the east. Among them, Zn, Ni, Cr, V, and Cu have consistent rankings in sediments and fuel oil (Table S4 and Figure S2). Ali and Abbas. (2006) have reported that coastal oil activities and oil spills can lead to elevated levels of TMs in the ocean. Therefore, we performed Spearman-Rho correlation analysis for TMs between seawater and fuel oil and the results showed a significant positive correlation ( $r = 0.79$ ,  $p < 0.05$ ) (Table S5). Combining the spatial distribution of TMs in seawater and sediments with the consistency of the spatial distribution of oil pollution, we suggest that oil pollution as a significant source of TMs is the main reason for this spatial heterogeneity. This is consistent with our subsequent identification of the effects of oil pollution on TMs in seawater through high-resolution time-series of W3 *Porites* coral skeletons.

### 4.2. Correlation analysis of TMs in coral samples

To observe the geochemical characteristics of TMs, Pearson correlations were determined for TMs in coral samples (Table 3). The positive correlation between TMs suggested that they may have originated from the same sources or have the same geochemical behaviors. Ni, V, Cr, Co, Cu, Mn, Fe, and Mo showed significant positive correlations ( $r \geq 0.70$ ,  $p < 0.01$ ), with particularly strong correlations for Cr, Co, Mn, Fe, and Mo ( $r > 0.92$ ,  $p < 0.01$ ). This indicated that these TMs shared the same geochemical behaviors or potential sources. Cd and Ba had high positive correlations ( $r = 0.56$ ,  $p < 0.01$ ). However, the positive correlations between Pb, Zn, Sr, and the other TMs were weaker, which may indicate that they have different sources of contamination or geochemical characteristics from the other TMs.

### 4.3. PCA of TMs in coral samples

To further identify the main geochemical behaviors of TMs and sources of contamination, PCA with maximum variance rotation was used to obtain a rotated component matrix (Table 4) and a rotated load space plot (Fig. 4). The PC1 with an eigenvalue of 7.09 accounts for 54.56% of the variance contribution and has a very high sample score. The rotated PC1 explains the geochemical behaviors or potential sources of Ni, V, Cr, Co, Cu, Mn, Fe, and Mo. The PC2 corresponds to Pb, Cd, and Ba with an eigenvalue of 1.75 and a variance contribution of 13.44%.

**Table 1**  
Percentile contents and statistics of TMs in W3 coral samples.

Element ( $\mu\text{g/g}$ )	Ni	V	Pb	Cr	Co	Zn	Cu	Cd	Mn	Fe ( $10^3$ )	Ba	Sr ( $10^3$ )	Mo
Minimum	0.01	0.06	0.11	0.01	0.09	0.05	<0.01	<0.01	0.46	<0.01	9.51	5.87	<0.01
10th percentile	0.03	0.08	0.23	0.11	0.09	0.05	<0.01	<0.01	0.65	<0.01	10.42	6.31	<0.01
25th percentile	0.07	0.10	0.29	0.21	0.11	0.05	<0.01	0.01	1.13	0.01	11.23	6.55	0.01
50th percentile	0.14	0.13	0.48	0.42	0.13	1.38	0.15	0.02	3.46	0.05	12.81	6.81	0.02
75th percentile	0.31	0.17	0.95	0.90	0.21	5.34	0.83	0.04	7.45	0.48	14.75	7.15	0.05
90th percentile	0.85	0.31	2.33	2.38	0.31	20.35	2.06	0.05	12.04	1.16	17.88	7.59	0.10
Maximum	18.14	1.59	14.75	31.67	8.05	147.70	38.68	0.18	445.50	54.39	32.11	8.24	3.04
Mean	0.60	0.17	1.15	1.19	0.26	7.32	1.12	0.03	10.09	0.93	13.73	6.89	0.08
St.D.	2.28	0.17	2.09	3.26	0.76	20.09	3.95	0.03	42.10	5.17	3.87	0.54	0.31
CV(%)	379	96	182	274	296	274	353	90	417	553	28	8	368

Table 2

TMs contents ( $\mu\text{g/g}$ ) in *Porites* corals from typical seas contaminated by oil activities.

Location	<i>Porites</i> species	Ni	V	Pb	Cr	Co	Zn	Cu	Cd	Mn	Fe ( $10^3$ )	References
W3	<i>Porites lutea</i>	0.60	0.17	1.15	1.19	0.26	7.32	1.12	0.03	10.09	0.93	This study
Kharg, Persian Gulf (Iran)	<i>Porites lobata</i>	2.68	0.12	0.25	0.46	0.26	21.86	4.15	0.01	1.28	–	Bolouki Kourandeh et al. (2021)
Hendourabi, Persian Gulf (Iran)	<i>Porites lobata</i>	2.53	0.08	0.07	0.61	0.20	1.54	5.46	0.01	0.82	–	
Red Sea (Saudi Arabia)	<i>Porites lutea</i>	0.15	7.58	51.00	–	–	9.28	0.83	0.06	6.67	0.03	Hanna and Muir (1990)
Bajo Caiman (Venezuela)	<i>Porites astreoides</i>	–	0.26	1.04	1.95	–	9.12	12.52	–	–	0.02	Bastidas and Garcia (1999)
Punta Brava (Venezuela)	<i>Porites astreoides</i>	–	0.31	0.21	0.80	–	10.67	16.33	–	–	0.06	
Gulf of Aqaba (Jordan)	<i>Porites</i> sp.	–	–	38.10	–	–	7.32	3.88	7.21	0.35	–	Al-Rousan et al. (2007)
Hurghada, Red Sea (Egypt)	<i>Porites solida</i>	6.34	–	12.30	–	3.57	11.30	3.56	1.31	9.21	0.09	Nour and Nouh (2020)
Ras Mohamed, Red Sea (Egypt)	<i>Porites solida</i>	2.68	–	6.10	–	2.17	5.20	1.60	1.22	4.21	0.06	
Quseir, Red Sea (Egypt)	<i>Porites lutea</i>	19.90	–	5.90	1.60	12.50	20.90	1.60	–	2.01	0.01	El-Sorogy et al. (2012)

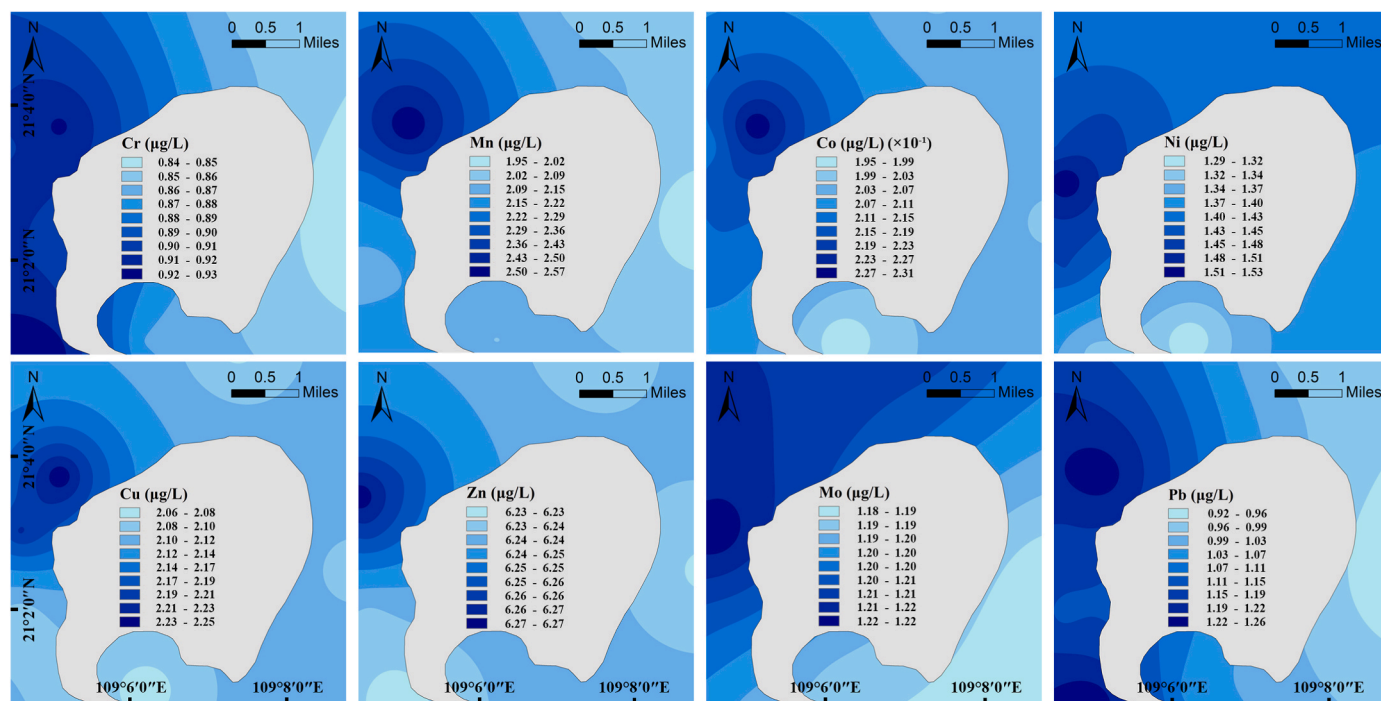


Fig. 2. Spatial distribution of TMs in the seawater around WZI.

The PC3 represents the geochemical behaviors and sources of Zn with an eigenvalue of 1.20 and a variance contribution of 9.23%. The PC4 corresponds to Sr and part of Ba with an eigenvalue of 1.18 and a variance contribution of 9.06%. As shown in Fig. 4A and C, TMs are divided into two groups, each explaining their respective natural influences. Fig. 4B and D show that these elements are subdivided into smaller groups, explaining the possible sources of these elements. Therefore, we will discuss the influences and sources separately.

#### 4.3.1. Seasonal patterns associated with the geochemical properties of elements

Shi et al. (2015) have reported the seasonality of seawater surface variation accompanied by the monsoon in the northern SCS. In Fig. 5, the obvious seasonal fluctuations of the PC1 scores can be observed from 2005 to 2007 AD. Therefore, to explore the seasonal variation pattern associated with elemental geochemical properties, we fitted some of the principal score intervals of the four principal components, in which the data distribution is relatively stable (small coefficient of variation) and less subject to human influence to SST. As shown in Fig. 6 and S5, except

for the PC1 scores, which were positively correlated with SST ( $r = 0.51$ ,  $p < 0.01$ ), the PC2, PC3, and PC4 scores were all negatively correlated with SST ( $r = -0.49$ ,  $p < 0.01$ ;  $r = -0.54$ ,  $p < 0.01$ ;  $r = -0.63$ ,  $p < 0.01$ ). High scores of PC1 all appeared in summer, while PC2, PC3, and PC4 all had high scores in winter. The influence of wind-borne currents was explored concerning the seasonal variation of the Beibu Gulf circulation (Figure S6). The circulation driven by the southwest monsoon in summer rotates counterclockwise. However, weak winds in the northern SCS in summer and unstable and unsustainable southwest monsoon are not favorable for the variation of metals. Furthermore, strong winds generated by tropical cyclones enhance the vertical mixing of seawater and stir up sediments (Srifer and Huber, 2007), thus changing the redox state and increasing the content of V, and Cu in seawater (Chen et al., 2015). The positive correlation between the PC1 scores and maximum wind speeds ( $r = 0.47$ ,  $p < 0.01$ ) (Fig. 7 and S6) may indicate that strong winds generated by tropical cyclones in summer drive higher levels of Ni, V, etc. in seawater. Therefore, it is reasonable to infer that SCS summer tropical cyclones are the main natural factor influencing the seasonal variation of PC1 (Ni, V, Cr, Co, Cu, Mn, Fe, and Mo).

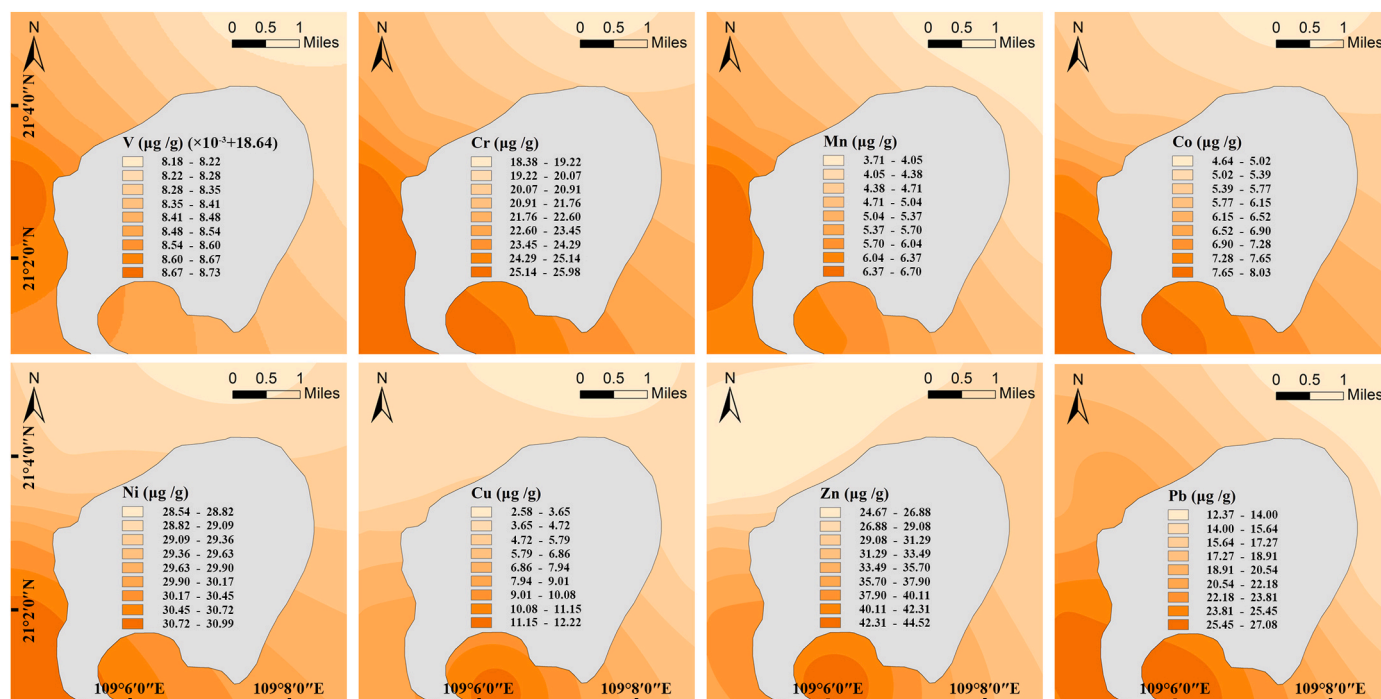


Fig. 3. Spatial distribution of TMs in the sediments around WZI.

Table 3

Pearson correlation coefficients  $\rho$  between TMs in W3 coral samples.

	Ni	V	Pb	Cr	Co	Zn	Cu	Cd	Mn	Fe	Ba	Sr	Mo
Ni	1												
V	0.70**	1											
Pb	-0.02	0.03	1										
Cr	0.75**	0.84**	0.13	1									
Co	0.78**	0.89**	-0.01	0.93**	1								
Zn	0.10	0.17	-0.03	0.28**	0.12	1							
Cu	0.74**	0.86**	0.04	0.87**	0.93**	0.18	1						
Cd	0.17	0.24*	0.29**	0.23*	0.14	0.26**	0.36**	1					
Mn	0.76**	0.89**	-0.01	0.92**	0.99**	0.10	0.93**	0.15	1				
Fe	0.76**	0.88**	-0.01	0.92**	0.99**	0.10	0.93**	0.14	0.99**	1			
Ba	0.19*	0.39**	0.28**	0.26**	0.20*	0.25**	0.32**	0.56**	0.20*	0.19*	1		
Sr	0.07	0.28**	-0.03	0.18	0.18	0.03	0.08	0.01	0.16	0.17	0.28**	1	
Mo	0.77**	0.84**	0.01	0.96**	0.93**	0.08	0.86**	0.18	0.92**	0.92**	0.20*	0.18	1

\*\*Correlation is significant at the 0.01 level (2-tailed).

\*Correlation is significant at the 0.05 level (2-tailed).

However, as the CVs for Sr are very low (Table 1) and normally distributed, Sr is mainly influenced by one specific factor. The incorporation of Sr in coral skeletons is temperature-dependent, with greater Sr incorporation at lower SST (Beck et al., 1992). Interestingly, as both Ba and Sr are alkaline earth elements, a similar effect exists for Ba (Shen et al., 1992). Sun et al. (2005) reported that the forcing of SST by the winter monsoons was well-represented in the *Porites* of the northern SCS. Meanwhile, the persistent strong southwestward currents in the northern Beibu Gulf near WZI, driven by winter monsoons (Figure S6), may have some influence on PC2, PC3, and PC4. Combining our results of fitting the PC2, PC3, and PC4 scores with SST, we suggest that the winter monsoons are the main natural factor for the seasonal variations of PC2 and PC3 (Pb, Cd, Ba, and Zn), while the seasonal variation of PC4 (Sr) is controlled by SST.

In addition, according to Chen et al. (2021) and Liang et al. (2021), the content of Cu and Cr in seawater/sediments around WZI was higher in summer than that in winter, while the seasonal differences of Pb, Cd, and Zn were reversed (Figure S8). It is noteworthy that the summers of its sampling years have been affected by tropical cyclones. These results

are consistent with the seasonal variation inferred from the PCA results in the time-series.

#### 4.3.2. PC1 associated with oil spills and marine oil extraction

The rotated PC1 explains the geochemical behavior and potential sources of Ni, V, Cr, Co, Cu, Mn, Fe, and Mo (Table 4). River input is an important source of Ni, V, and Mn in the ocean (Chen et al., 2015; Revels et al., 2021). The TMs input from rivers to the ocean is rapidly adsorbed due to the strong adsorption capacity of estuarine sediments (Miranda et al., 2021). However, as WZI is far from the mainland, it is difficult to receive land-sourced metals from rivers. Therefore, the riverine input metals are insignificant in the high-resolution monthly variation. Considering that Ni and V are very abundant elements in oil, coastal oil activities and oil spills can lead to the enrichment of TMs in marine ecosystems (Ali and Abbas, 2006). Interestingly, the Weizhou oil field has been in production since 1986, and a complex series of oil facilities have been built in the sea with an oil pipeline leak occurred in 2002. Therefore, it is reasonable to infer that oil pollution imported Ni, V, Cr, Co, Cu, Mn, Fe, and Mo as micronutrients into seawater, mainly enriched

**Table 4**

Principal component factor scores with Varimax rotation solution of TMs in W3 coral samples.

	Principal component extraction with varimax rotation solution			
	1	2	3	4
Eigenvalue	7.09	1.75	1.20	1.18
% of variance	54.56	13.44	9.23	9.06
Ni	<b>0.83</b>	0.04	0.05	-0.03
V	<b>0.89</b>	0.15	0.10	0.23
Pb	-0.01	<b>0.78</b>	-0.36	-0.12
Cr	<b>0.94</b>	0.14	0.13	0.06
Co	<b>0.99</b>	0.01	0.03	0.07
Zn	0.09	0.10	<b>0.90</b>	-0.01
Cu	<b>0.93</b>	0.19	0.14	-0.01
Cd	0.14	<b>0.76</b>	0.35	-0.03
Mn	<b>0.99</b>	0.02	0.01	0.07
Fe	<b>0.98</b>	0.01	0.01	0.07
Ba	0.16	<b>0.69</b>	0.30	0.41
Sr	0.11	0.01	-0.03	<b>0.96</b>
Mo	<b>0.95</b>	0.05	-0.01	0.07

The bolds represent the number >0.6.

in the bottom seawater and sediments. The enhanced vertical mixing of seawater under the influence of strong winds generated by tropical cyclones in summer has led to the release of these elements, enriched through oil pollution, from the sediments into the surface seawater (Sriver and Huber, 2007).

Although, during 2008–2015 AD, the strong winds still had seasonal effects on these elements in sediments. However, unlike the geochemical behavior in 2005–2007 AD, the PC1 scores lost significant correlation with maximum wind speeds in 2008–2015 AD, suggesting that the steep rise in the PC1 scores during this period seemed to be caused by sudden anthropogenic pollution rather than strong winds. (Figure S9 and S10). Previous studies have shown that V and Ni in coral skeletons may provide a stable proxy for oil pollution (Guzman and Jarvis, 1996; Wu et al., 2022). In recent years, oil spill events and pollution from oil activities in

the Beibu Gulf have become increasingly frequent with the increase in marine oil field drilling platforms and ship shipping. In addition, we measured TMs in fuel oil leaked from the sinking of the cargo ship in the waters around WZI (Figure S2). The results showed that the fuel oil contained abundant Ni, V, Cr, Co, Cu, Mn, and Mo. Moreover, the W3 *Porites lutea* was significantly and positively correlated with the TMs (Cr, Mn, Co, Ni, Cu, Zn and Mo) in fuel oil ( $r = 0.79$ ,  $p < 0.05$ ) (Table S5), despite the different sampling times. Therefore, we investigated the history of oil pollution around WZI in the Beibu Gulf and found that several serious marine oil spills occurred near WZI from 2008 to 2015 AD. The multiple abrupt peaks of PC1 coincided with the oil spills around WZI in 2009, 2011, 2012, and 2014 AD as recorded in the annual environmental quality bulletin of Guangxi Zhuang Autonomous Region (Fig. 5). Furthermore, in the event of a marine oil spill, the  $\delta^{13}\text{C}$  in seawater will be sharply and negatively displaced. Xu et al. (2018) have already reported that several sharp negative shifts of  $\delta^{13}\text{C}$  in seawater from 2005 to 2015 AD were attributed to marine oil spills, which corresponds exactly to the four mutation peaks of PC1 in this study (Fig. 5), further validating the effects of these marine oil spills on Ni, V, Cr, Co, Cu, Mn, Fe, and Mo in coral skeletons. In addition, marine oil fields also deliver TMs to the marine environment during the exploration and extraction process (Hoffmann and Borrok, 2020). Throughout the development history of the Weizhou field, we found that the peak mutations of the PC1 scores in 2010, 2013, and 2015 AD corresponded to the development times of WZ6-8 and WZ11-1 N, WZ6-12 and WZ12-8, and Phase II WZ12-2 and Phase II WZ11-4 N fields, respectively (Fig. 5). Notably, how long TMs from marine oil spills and oil extraction remain in the surface seawater could affect their recordation by coral skeletons. Calculating the peak interval of the PC1 score, the time range of marine oil spills and oil extraction affecting TMs in surface seawater ranges from 1 to 3 months, with an average of 1.4 months.

#### 4.3.3. PC2 associated with oil extraction and oil usage

PC2 corresponds to Pb, Cd, and Ba (Table 4). Dang et al. (2015) reported that shipping fuel oil combustion around the harbor is a source of

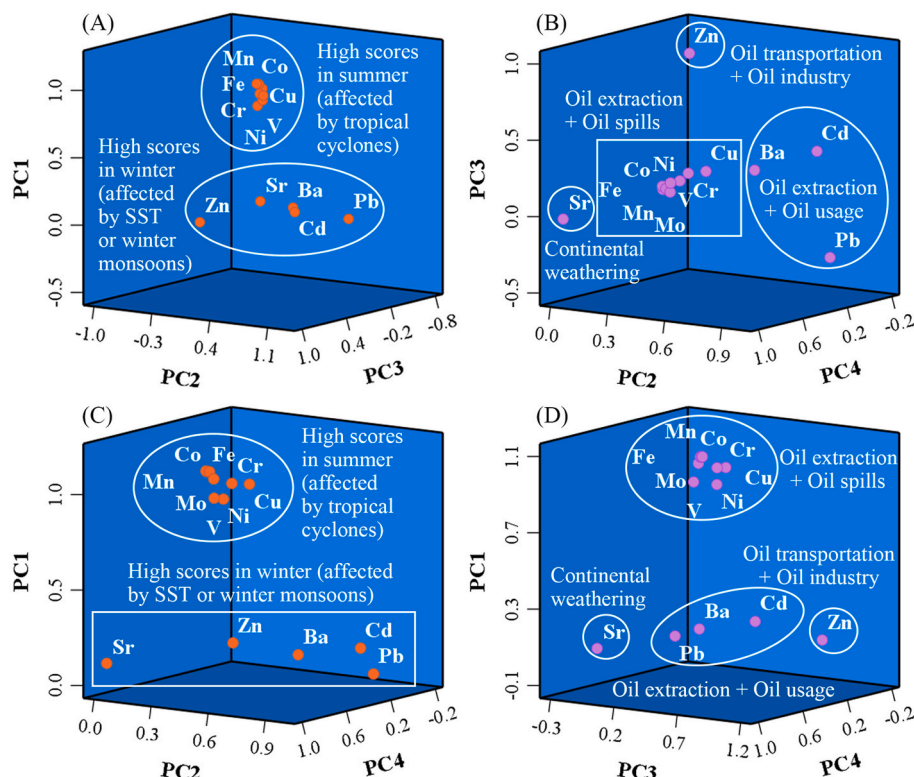
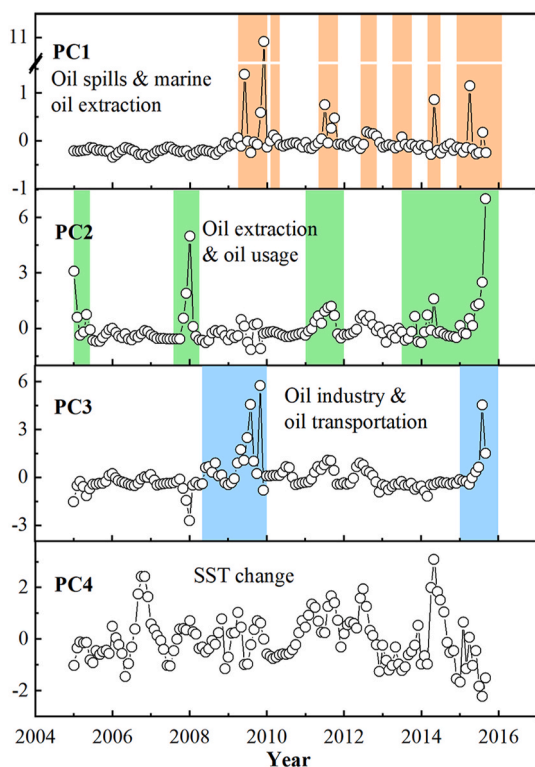


Fig. 4. Loading 3-D plot for TMs produced from PCA with Varimax rotation solution.



**Fig. 5.** A principal score on the principal components with Varimax rotation solution. The yellow background represents the oil spills and marine oil exploitation recorded in the annual bulletin of marine environmental quality of Guangxi Zhuang Autonomous Region, the green background represents port dredging and wharf construction, and the blue background represents the oil industry and oil transportation. Data sources: Marine Environment Bulletin of Guangxi Zhuang Autonomous Region.

dissolved Pb and that sediments resuspension during dredging significantly increases the Pb content in seawater. Sudden increases in Cd and Ba contents in surface seawater have also been associated with sediments resuspension caused by dredging (Deepthi et al., 2014; Esslemont et al., 2004). Examination of the dredging history around WZI revealed that dredging had occurred around WZI in 2005, 2007–2008, 2011–2012, and 2014–2016 AD, which corresponded to the peak of

abrupt changes in the PC2 scores (Fig. 5). Furthermore, Yang et al. (2015) have reported that Pb, Cd, and Ba discharged from oil extraction around WZI are susceptible to enrichment in sediments during migration. Therefore, we reasonably infer that PC2 explains the dredging-driven sediments re-release of Pb, Cd, and Ba originated from oil extraction and usage.

#### 4.3.4. PC3 associated with the oil industry and oil transportation

To process crude oil from the nearby Weizhou oilfield, a crude oil terminal treatment plant and an oil terminal have been constructed on the northwest side of WZI. Whereas Zn has proven to be an important indicator for the oil industry and transportation (Cram et al., 2006). Interestingly, according to the spatial distribution characteristics of Zn in seawater in Fig. 2, its highest level also occurs near crude oil terminal treatment plants and oil terminals. Crude oil produced from the Weizhou oilfield is directly transported through a subsea pipeline to the Weizhou terminal plant for treatment. The amount of crude oil treated at the Weizhou terminal plant is dependent on the annual production of crude oil from the Weizhou oilfield. Therefore, we investigated the relationship between the PC3 scores and the annual production of crude oil from the Weizhou field (Fig. 8). As shown in Fig. 8, the temporal changes in PC3 scores coincide with the decline in crude oil production

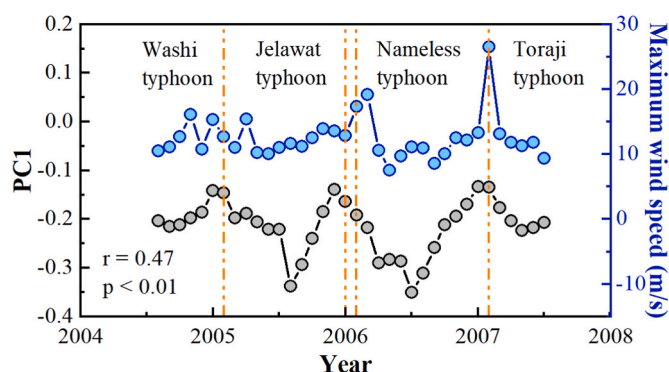


**Fig. 7.** Plot showing relationships between the PC1 and maximum wind speed in WZI waters between 2005 and 2007 AD. The yellow dashed line represents the tropical cyclones affecting the waters of WZI. Data sources: the maximum wind speed dates in WZI from the Greenhouse data sharing platform (<http://datasheshiyuanyi.com/>); the tropical cyclones dates from the Central Weather Bureau Typhoon Network (<http://typhoon.nmc.cn/web.html>).

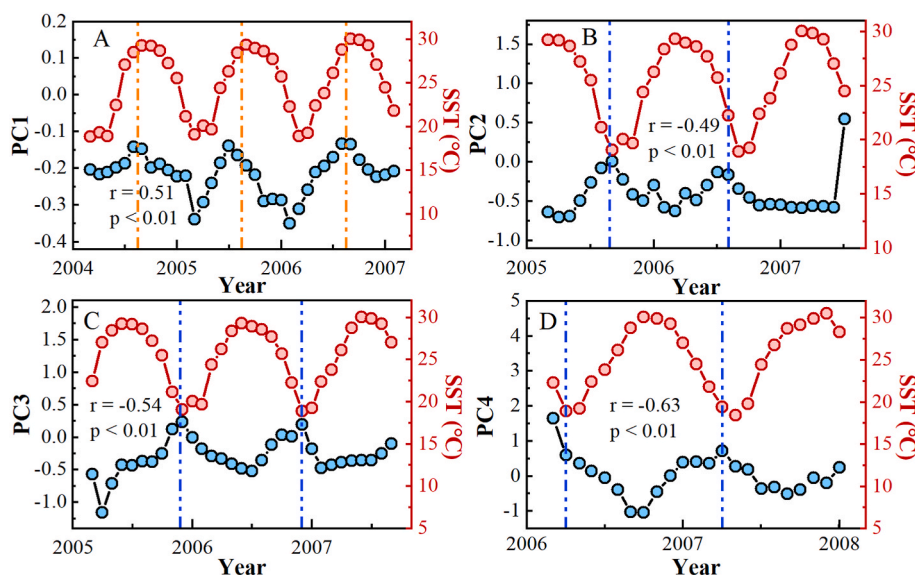


**Fig. 6.** Plots of partial principal scores of each principal component with SST (PC1 principal score from January 2005 to December 2007 (A), PC2 principal score from July 2005 to November 2007 (B), PC3 principal score from April 2005 to October 2007 (C), and PC4 principal score from December 2006 to October 2008 (D) plotted with SST). The yellow dotted line represents a high score in the summer and the blue dotted line represents a high score in the winter. Data sources: the SST dates around WZI from NOAA (National Oceanic and Atmospheric Administration) Physical Sciences Laboratory (<https://psl.noaa.gov/data/index.html>).

in 2007 AD and the rise in 2008–2010 AD. Coincidentally, the abrupt change peak of PC3 scores in 2015 AD also corresponds to the rapid increase in annual crude oil production in 2015 AD. Simultaneously, Tankers need to discharge significant amounts of Zn-containing ballast water before loading oil at the Weizhou oil terminal. Therefore, these results suggest that Zn contamination in W3 coral skeletons originated from discharges from the oil industry at the Weizhou crude oil terminal treatment plant and ballast water from tankers at the oil transportation terminal.

#### 4.4. Principal component analysis with multivariate linear regression

PCA can be used to explain the geochemical characteristics or potential sources of TMs in coral skeletons. From the above PCA, it is clear that four principal components explain 86.3% of the variation in TMs in W3 coral. To further understand the influence or contribution of the sources or geochemical behavior represented by each principal component on TMs, we combined the PCA model with a multivariate linear regression (MLR) model and performed a stepwise regression of TMs using the four principal component scores and quantified the coefficients using MLR to calculate the contribution of each source to TMs (Fig. 9). The method (PCA-MLR) has been previously used to assess the source and distributional contribution to the geochemical behavior of TMs in surface sediments (Song et al., 2011). As shown in Fig. 9, over 60% of Ni, V, Cr, Co, Cu, Mn, Fe, and Mo were ultimately sourced from marine oil spills and marine oil extraction. A further 7.8% of Zn, 10.6% of Cd, 10.1% of Ba, and 9.8% of Sr are influenced by oil spills and oil extraction. The contribution rates of oil extraction and oil usage to Pb, Cd, and Ba were 61.5%, 59.3%, and 44.4%, respectively. The oil industry and oil transportation contributed 81.9% of Zn, and a further 27.6% of Cd was also associated with the oil industry and oil transportation. In addition, the SST variation represented by PC4 mainly affected Sr, while 17.1% of V and 26.3% of Ba were also associated with SST variation. In summary, oil pollution contributed significantly to most of the selected TMs, accounting for 77.2%.

## 5. Conclusions

The present study demonstrates that the changes in TMs contents in surface seawater around WZI in the northern SCS are closely related to oil activities. In this study, the spatial distribution characteristics of TMs in seawater and sediments suggest that high values of Cr, Mn, Co, Ni, Cu, Zn, and Mo in seawater and V, Cr, Mn, Co, and Ni in sediments are

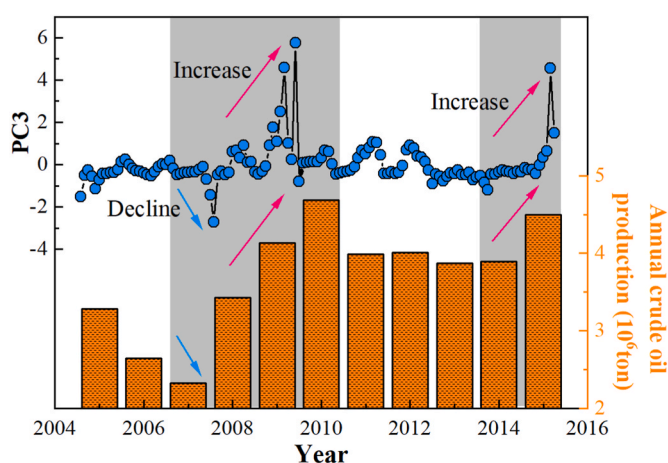


Fig. 8. Plot showing the relationship between annual crude oil production of the Weizhou oilfield and the PC3 scores between 2005 and 2015 AD. The blue histogram represents the annual crude oil production of the Weizhou oilfield. Data sources: the crude oil production in the Weizhou oilfield dates from Guangxi Statistical Yearbook.

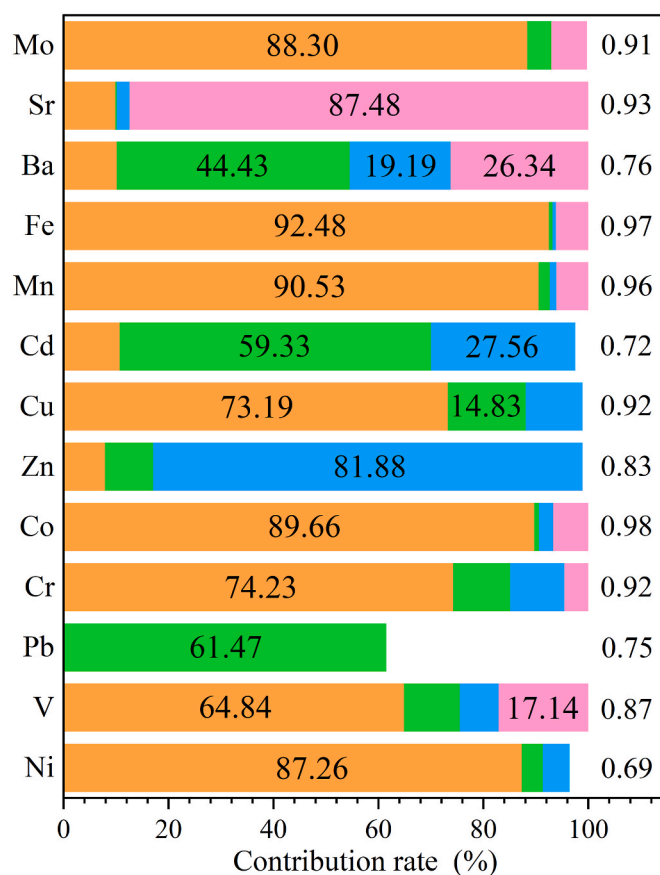


Fig. 9. Contribution apportionment of influence factors of TMs in W3 coral samples. The yellow background represents the oil spills and marine oil extraction, the green background represents oil extraction and oil usage, the blue background represents oil industry and oil transportation, and the pink background represents SST. The value of R<sup>2</sup> is marked to the right of each column.

associated with oil pollution. The PCA-MLR results of coral samples show that the total contribution of oil pollution as a source to TMs in surface seawater was 77.2%, where the residence time of TMs released from oil spills in surface seawater was approximately 1.4 months. In addition, strong winds generated by summer tropical cyclones were the primary natural factor influencing the seasonal variability of Ni, V, Cr, Co, Cu, Mn, Fe, and Mo in surface seawater, while the seasonal variations of Pb, Cd, Ba, and Zn were impacted by winter monsoons, and Sr was controlled by SST. These findings provide valuable reference and insight into accurately identifying and quantifying TMs released from marine oil pollution using corals as a recording vehicle, and estimating the duration of the impact on surface seawater. In future work, the applicability of coral skeletons as a recording tool need to be explored in other oil-polluted seas.

#### Credit author statement

**Sirong Xie:** Investigation, Formal analysis, Writing-Original draft preparation; **Wei Jiang:** Conceptualization, Investigation, Methodology, Formal analysis, Writing-Reviewing and Editing, Funding Acquisition, Resource; **Chunmei Feng:** Investigation, Methodology; **Yinan Sun:** Methodology, Data curation; **Yansong Han:** Investigation, Methodology; **Yuwen Xiao:** Investigation, Methodology; **Chaoshuai Wei:** Methodology, Data Curation; **Kefu Yu:** Data curation, Funding Acquisition, Resource, Supervision.

## Declaration of competing interest

The authors declare that they have no known competing financial interests or personal relationships that could have appeared to influence the work reported in this paper.

## Data availability

Data will be made available on request.

## Acknowledgments

This research was supported by the National Natural Science Foundation of China (Grant Nos. 42030502, 41976059, and 42090041) and the project was supported by the Innovation Group Project of Southern Marine Science and Engineering Guangdong Laboratory (Zhuhai) (No. 311019006/311020006). Thanks are due to the responsible editor and two anonymous reviewers for their critical reviews and constructive comments, which helped us improve significantly our paper.

## Appendix A. Supplementary data

Supplementary data to this article can be found online at <https://doi.org/10.1016/j.chemosphere.2023.139632>.

## References

- Ahmad, D., Hafizan, J., Kamaruzzaman, Y., Mohammad, A., Che, N., Fazureen, A., Ismail, Z., Syahril, H., Nur, H., 2015. Oil spill related heavy metal: a review. *Malaysian J. Anal. Sci.* 19 (6), 1348–1360.
- Al-Rousan, S.A., Al-Shioul, R.N., Al-Horani, F.A., Abu-Hilal, A.H., 2007. Heavy metal contents in growth bands of Porites corals: record of anthropogenic and human developments from the Jordanian Gulf of Aqaba. *Mar. Pollut. Bull.* 54 (12), 1912–1922. <https://doi.org/10.1016/j.marpolbul.2007.08.014>.
- Alharbi, T., Al-Kahtany, K., Nour, H.E., Giacobbe, S., El-Sorogy, A.S., 2022. Contamination and health risk assessment of arsenic and chromium in coastal sediments of Al-Khobar area, Arabian Gulf, Saudi Arabia. *Mar. Pollut. Bull.* 185 (A), 1–6. <https://doi.org/10.1016/j.marpolbul.2022.114255>.
- Ali, M.F., Abbas, S., 2006. A review of methods for the demetallization of residual fuel oils. *Fuel Process. Technol.* 87 (7), 573–584. <https://doi.org/10.1016/j.fuproc.2006.03.001>.
- Amorosi, A., 2012. Chromium and nickel as indicators of source-to-sink sediment transfer in a Holocene alluvial and coastal system (Po Plain, Italy). *Sediment. Geol.* 280, 260–269. <https://doi.org/10.1016/j.sedgeo.2012.04.011>.
- Bastidas, C., Garcia, E., 1999. Metal content on the reef coral Porites astreoides: an evaluation of river influence and 35 years of chronology. *Mar. Pollut. Bull.* 38 (10), 899–907. [https://doi.org/10.1016/S0025-326X\(99\)00089-2](https://doi.org/10.1016/S0025-326X(99)00089-2).
- Beck, J.W., Edwards, R.L., Ito, E., Taylor, F.W., Recy, J., Rougerie, F., et al., 1992. Sea-surface temperature from coral skeletal strontium/calcium ratios. *Science* (New York, N.Y.) 257 (5070), 644–647. <https://doi.org/10.1126/science.257.5070.644>.
- Bolouki Kourandeh, M., Nabavi, S.M.B., Shokri, M.R., Ghanemi, K., Feng, Y., 2021. Trace metal content in annually banded scleractinian coral 'Porites lobata' across the northern Persian Gulf. *Environ. Sci. Pollut. Control Ser.* 28 (43), 61008–61020. <https://doi.org/10.1007/s11356-021-14938-8>.
- Breuer, E., Stevenson, A.G., Howe, J.A., Carroll, J., Shimmield, G.B., 2004. Drill cutting accumulations in the Northern and Central North Sea: a review of environmental interactions and chemical fate. *Mar. Pollut. Bull.* 48 (1–2), 12–25. <https://doi.org/10.1016/j.marpolbul.2003.08.009>.
- Bu-Olayan, A.H., Subrahmanyam, M.N.V., Al-Sarawi, M., Thomas, B.V., 1998. Effects of the Gulf War oil spill about trace metals in water, particulate matter, and PAHs from the Kuwait coast. *Environ. Int.* 24 (7), 789–797. [https://doi.org/10.1016/S0160-4120\(98\)00056-7](https://doi.org/10.1016/S0160-4120(98)00056-7).
- Chen, J., Zhang, W., Wan, Z., Li, S., Huang, T., Fei, Y., 2019. Oil spills from global tankers: status review and future governance. *J. Clean. Prod.* 227, 20–32. <https://doi.org/10.1016/j.jclepro.2019.04.020>.
- Chen, L., Dai, S., Lei, F., Zhang, T., Xu, Y., Liang, Q., Huang, X., Liu, X., 2021. Study on heavy metal pollution in coastal waters of Weizhou Island. *J. Guangxi Acad. Sci.* 37, 37–45.
- Chen, X., Wei, G., Deng, W., Liu, Y., Sun, Y., Zeng, T., Xie, L., 2015. Decadal variations in trace metal concentrations on a coral reef: evidence from a 159 year record of Mn, Cu, and V in a Porites coral from the northern South China Sea. *J. Geophys. Res.-Oceans* 120 (1), 405–416. <https://doi.org/10.1002/2014JC010390>.
- Cram, S., Ponce De Leon, C.A., Fernandez, P., Sommer, I., Rivas, H., Morales, L.M., 2006. Assessment of trace elements and organic pollutants from a marine oil complex into the coral reef system of Cayo Arcas, Mexico. *Environ. Monit. Assess.* 121 (1–3), 127–149. <https://doi.org/10.1007/s10661-005-9111-7>.
- Dang, D.H., Schaefer, J., Brach-Papa, C., Lenoble, V., Durrieu, G., Dutrich, L., et al., 2015. Evidencing the impact of coastal contaminated sediments on mussels through Pb stable isotopes composition. *Environ. Sci. Technol.* 49 (19), 11438–11448. <https://doi.org/10.1021/acs.est.5b01893>.
- Deepthi, K., Natesan, U., Muthulakshmi, A.L., Ferrer, V.A., Venugopalan, V.P., Narasimhan, S.V., 2014. Heavy metals in nearshore sediments of Kalpakkam, southeast coast of India. *Environ. Earth Sci.* 72 (3), 717–729. <https://doi.org/10.1007/s12665-013-2996-5>.
- Duleba, W., Gubitoso, S., Alves Martins, M.V., Teodoro, A.C., Pregolato, L.A., Prada, S.M., 2019. Evaluation of contamination by potentially toxic elements (PTE) of sediments around the petroleum terminal pipeline "dutos e terminais do centro sul (DTCS)", SP, Brazil. *J. Sediment. Environ.* 4 (4), 387–402. <https://doi.org/10.12957/jse.2019.46539>.
- Dong, Y., Liu, Y., Hu, C., MacDonald, I., Lu, Y., 2022a. Chronic oiling in global oceans. *Science* 376 (6599), 1300–1304. <https://doi.org/10.1126/science.abm5940>.
- Dong, H., Su, J., Zhou, S., Ling, S., Chen, G., Wang, F., 2022b. Investigating the contents and sources of heavy metals in the winter season in Xisha waters of South China Sea. *J. Trop. Oceanography* 1–8.
- El-Sorogy, A.S., Mohamed, M.A., Nour, H.E., 2012. Heavy metals contamination of the Quaternary coral reefs, Red Sea coast, Egypt. *Environ. Earth Sci.* 67 (3), 777–785. <https://doi.org/10.1007/s12665-012-1535-0>.
- Esslemont, G., Russell, R.A., Maher, W.A., 2004. Coral record of harbour dredging: townsville, Australia. *J. Mar. Syst.* 52 (1–4), 51–64. <https://doi.org/10.1016/j.jmarsys.2004.01.005>.
- Gong, S., Liu, W., Li, Y., Zhang, J., Chen, C., Fu, J., 2020. Distribution characteristics and source tracing of petroleum hydrocarbons in the northeastern South China Sea. *Chem. Lett.* 31 (10), 2854–2858. [https://doi.org/10.1016/S0025-326X\(99\)00183-6](https://doi.org/10.1016/S0025-326X(99)00183-6).
- Guzman, H.M., Jarvis, K.E., 1996. Vanadium century record from Caribbean reef corals: a tracer of oil pollution in Panama. *Ambio* 25 (8), 523–526. <http://www.jstor.org/stable/4314533>.
- Hanna, R.G., Muir, G.L., 1990. Red sea corals as biomonitors of trace metal pollution. *Environ. Monit. Assess.* 14 (2–3), 211–222. <https://doi.org/10.1007/BF00677917>.
- Hoffmann, A.A., Borrok, D.M., 2020. The geochemistry of produced waters from the Tuscaloosa Marine Shale, USA. *Appl. Geochem.* 116. <https://doi.org/10.1016/j.apgeochem.2020.104568>.
- Inoue, M., Suzuki, A., Nohara, M., Kan, H., Edward, A., Kawahata, H., 2004. Coral skeletal tin and copper concentrations at Pohnpei, Micronesia: possible index for marine pollution by toxic anti-biofouling paints. *Environ. Pollut.* 129 (3), 399–407. <https://doi.org/10.1016/j.envpol.2003.11.009>.
- Jiang, W., Yu, K.F., Song, Y.X., Zhao, J.X., Feng, Y.X., Wang, Y.H., Xu, S.D., 2017. Coral trace metal of natural and anthropogenic influences in the northern South China Sea. *Sci. Total Environ.* 607, 195–203. <https://doi.org/10.1016/j.scitotenv.2017.06.105>.
- Jiang, W., Yu, K., Wang, N., Yang, H., Yang, H., Xu, S., et al., 2020. Distribution coefficients of trace metals between modern coral-lattices and seawater in the northern South China Sea: species and SST dependencies. *J. Asian Earth Sci.* 187. <https://doi.org/10.1016/j.jseas.2019.104082>.
- King, S.M., Leaf, P.A., Olson, A.C., Ray, P.Z., Tarr, M.A., 2014. Photolytic and photocatalytic degradation of surface oil from the Deepwater Horizon spill. *Chemosphere* 95, 415–422. <https://doi.org/10.1016/j.chemosphere.2013.09.060>.
- Kinzie, R.A., Buddemeier, R.W., 1996. Reefs happen. *Global Change Biol.* 2 (6), 479–494. <https://doi.org/10.1111/j.1365-2486.1996.tb00062.x>.
- Lewis, S.E., Lough, J.M., Cantin, N.E., Matson, E.G., Kinsley, L., Bainbridge, Z.T., Brodie, J.E., 2018. A critical evaluation of coral Ba/Ca, Mn/Ca and Y/Ca ratios as indicators of terrestrial input: new data from the Great Barrier Reef, Australia. *Geochim. Cosmochim. Acta* 237, 131–154. <https://doi.org/10.1016/j.gca.2018.06.017>.
- Li, K., Yu, H., Yan, J., Liao, J., Iop, 2020. Analysis of offshore oil spill pollution treatment technology. In: Paper Presented at the 4th International Workshop on Renewable Energy and Development (IWRED). *Electr. Network*, p. 510. <https://doi.org/10.1088/1755-1315/510/4/042011>.
- Li, J., Ting, Z., Liu, L., Xiong, J., Shi, H., Wang, J., 2022. Transfer and accumulation of trace elements in seawater, sediments, green turtle forage, and eggshells in the Xisha Islands, South China Sea. *Environ. Sci. Pollut. Control Ser.* 29, 50832–50844. <https://doi.org/10.1007/s11356-022-19354-0>.
- Liang, Q., Liu, X., Xu, Y., Zhang, T., Lei, F., Chen, L., Huang, X., Dai, S., 2021. Quality status and evaluation of heavy metals in the sea around Weizhou Island. *Guangxi Sci.* 28, 136–144.
- Liu, Z., Liu, J., Zhu, Q., Wu, W., 2012. The weathering of oil after the Deepwater Horizon oil spill: insights from the chemical composition of the oil from the sea surface, salt marshes and sediments. *Environ. Res. Lett.* 7 (3). <https://doi.org/10.1088/1748-9326/7/3/035302>.
- Miranda, L.S., Wijesiri, B., Ayoko, G.A., Egodawatta, P., Goonetilleke, A., 2021. Water-sediment interactions and mobility of heavy metals in aquatic environments. *Water Res.* 202. <https://doi.org/10.1016/j.watres.2021.117386>.
- Neira, P., Romero-Freire, A., Basallote, M., Qiu, H., Cobelo-Garcia, A., Canovas, C., 2022. Review of the concentration, bioaccumulation, and effects of lanthanides in marine systems. *Front. Mar. Sci.* 9. <https://doi.org/10.3389/fmars.2022.920405>.
- Nguyen, A.D., Zhao, J.X., Feng, Y.X., Hu, W.P., Yu, K.F., Gasparon, M., 2013. Impact of recent coastal development and human activities on Nha Trang Bay, Vietnam: evidence from a Porites lutea geochemical record. *Coral Reefs* 32 (1), 181–193. <https://doi.org/10.1007/s00338-012-0962-4>.
- Nour, H.E.S., Nour, E.S., 2020. Using coral skeletons for monitoring of heavy metals pollution in the Red Sea Coast, Egypt. *Arabian J. Geosci.* 13 (10). <https://doi.org/10.1007/s12517-020-05308-8>.
- Nour, H.E., Alshehri, F., Sahour, H., El-Sorogy, A.S., Tawfik, M., 2022. Assessment of heavy metal contamination and health risk in the coastal sediments of Suez Bay, Gulf of Suez, Egypt. *J. Afr. Earth Sci.* 195, 1–9. <https://doi.org/10.1016/j.jafrearsci.2022.104663>.

- Ortiz-Ojeda, C.P., Rázuri-Esteves, V.F., 2021. Baseline study to determine the implementation area of an oily waste management system for artisanal fishing vessels. *Environ. Monit. Assess.* 193 (2), 64. <https://doi.org/10.1007/s10661-021-08845-1>.
- Passow, U., Overton, E.B., 2021. The complexity of spills: the fate of the deepwater horizon oil. *Ann. Rev. Mar. Sci.* 13, 109–136. <https://doi.org/10.1146/annurev-marine-032320-095153>.
- Prouty, N.G., Hughen, K.A., Carilli, J., 2008. Geochemical signature of land-based activities in Caribbean coral surface samples. *Coral Reefs* 27 (4), 727–742. <https://doi.org/10.1007/s00338-008-0413-4>.
- Revels, B.N., Rickli, J., Moura, C.A.V., Vance, D., 2021. Nickel and its isotopes in the Amazon Basin: the impact of the weathering regime and delivery to the oceans. *Geochem. Cosmochim. Acta* 293, 344–364. <https://doi.org/10.1016/j.gca.2020.11.005>.
- Saha, N., Webb, G.E., Zhao, J.-X., 2016. Coral skeletal geochemistry as a monitor of inshore water quality. *Sci. Total Environ.* 566, 652–684. <https://doi.org/10.1016/j.scitotenv.2016.05.066>.
- Shen, G.T., Boyle, E.A., 1987. Lead in corals: reconstruction of historical industrial fluxes to the surface ocean. *Earth Planet Sci. Lett.* 82 (3–4) [https://doi.org/10.1016/0012-821X\(87\)90203-2](https://doi.org/10.1016/0012-821X(87)90203-2).
- Shen, G.T., Cole, J.E., Lea, D.W., Linn, L.J., McConnaughey, T.A., Fairbanks, R.G., 1992. Surface ocean variability at Galapagos from 1936–1982: calibration of geochemical tracers in corals. *Paleoceanography* 7 (5), 563–588. <https://doi.org/10.1029/92PA01825>.
- Shi, R., Guo, X.Y., Wang, D.X., Zeng, L.L., Chen, J., 2015. Seasonal variability in coastal fronts and its influence on sea surface wind in the Northern South China Sea. *Deep Sea Res. Part II Top. Stud. Oceanogr.* 119, 30–39. <https://doi.org/10.1016/j.dsr2.2013.12.018>.
- Song, Y., Ji, J., Yang, Z., Yuan, X., Mao, C., Frost, R.L., Ayoko, G.A., 2011. Geochemical behavior assessment and apportionment of heavy metal contaminants in the bottom sediments of lower reach of Changjiang River. *Catena* 85 (1), 73–81. <https://doi.org/10.1016/j.catena.2010.12.009>.
- Song, Y., Yu, K., Zhao, J., Feng, Y., Shi, Q., Zhang, H., et al., 2014. Past 140-year environmental record in the northern South China Sea: evidence from coral skeletal trace metal variations. *Environ. Pollut.* 185, 97–106. <https://doi.org/10.1016/j.envpol.2013.10.024>.
- Spooner, P., Robinson, L., Hemsing, F., Morris, P., Stewart, J., 2018. Extended calibration of cold-water coral Ba/Ca using multiple genera and co-located measurements of dissolved barium concentration. *Chem. Geol.* 499, 100–110. <https://doi.org/10.1016/j.chemgeo.2018.09.012>.
- Srifer, R., Huber, M., 2007. Observational evidence for an ocean heat pump induced by tropical cyclones. *Nature* 447 (7144), 577–580. <https://doi.org/10.1038/nature05785>.
- Sun, D.H., Gagan, M.K., Cheng, H., Scott-Gagan, H., Dykoski, C.A., Edwards, R.L., Su, R. X., 2005. Seasonal and interannual variability of the Mid-Holocene East Asian monsoon in coral delta O-18 records from the South China Sea. *Earth Planet Sci. Lett.* 237 (1–2), 69–84. <https://doi.org/10.1016/j.epsl.2005.06.022>.
- Tao, W., Li, H., Peng, X., Zhang, W., Lou, Q., Gong, J., Ye, J., 2021. Characteristics of heavy metals in seawater and sediments from daya Bay (South China): environmental fates, source apportionment and ecological risks. *Sustainability* 13, 10237. <https://doi.org/10.3390/su131810237>.
- Vaz, A.C., Faillettaz, R., Paris, C.B., 2021. A coupled Lagrangian-earth system model for predicting oil photooxidation. *Front. Mar. Sci.* 8, 576747 <https://doi.org/10.3389/fmars.2021.576747>.
- Veron, J., 2000. *Corals of the World*. Australia Institute of Marine Science, Townsville, pp. 1–773.
- Wang, Q., Peng, F., Chen, Y.Q., Jin, L., Lin, J., Zhao, X., et al., 2019. Heavy metals and PAHs in an open fishing area of the East China Sea: multimedia distribution, source diagnosis, and dietary risk assessment. *Environ. Sci. Pollut. Control Ser.* 26 (21), 21140–21150. <https://doi.org/10.1007/s11356-019-05355-z>. Article.
- Wei, X., He, L., Xie, Y., Chen, Y., Chen, Y., 2013. Direct determination of 7 elements in seawater by inductively coupled plasma mass spectrometry with collision reaction interface. *Gunagxi Sci.* 20 (3), 230–233.
- Wu, X., Jiang, W., Yu, K., Xu, S., Yang, H., Wang, N., et al., 2022. Coral-inferred historical changes of nickel emissions related to industrial and transportation activities in the Beibu Gulf, northern South China Sea. *J. Hazard Mater.* 424 <https://doi.org/10.1016/j.jhazmat.2021.127422>.
- Xu, S., Yu, K., Wang, Y., Liu, T., Jiang, W., Wang, S., Chu, M., 2018. Oil spill recorded by skeletal delta C-13 of Porites corals in Weizhou island, Beibu Gulf, northern South China sea. *Estuar. Coast Shelf Sci.* 207, 338–344. <https://doi.org/10.1016/j.ecss.2018.04.031>.
- Yang, H., Wang, S., Yu, K., Huang, X., Zhang, R., Wang, Y., Guo, S., 2017. Pollution characteristics of heavy metals in seawater of coral growing regions in the northern South China sea. *Ecol. Environ. Sci.* 26 (2), 253–260.
- Yang, J., Wang, W., Zhao, M., Chen, B., Dada, O., Chu, Z., 2015. Spatial distribution and historical trends of heavy metals in the sediments of petroleum producing regions of the Beibu Gulf, China. *Mar. Pollut. Bull.* 91 (1), 87–95. <https://doi.org/10.1016/j.marpolbul.2014.12.023>.
- Yu, Z., Lin, Q., Gu, Y., Du, F., Wang, X., Shi, F., et al., 2019. Bioaccumulation of polycyclic aromatic hydrocarbons (PAHs) in wild marine fish from the coastal waters of the northern South China Sea: risk assessment for human health. *Ecotoxicol. Environ. Saf.* 180, 742–748. <https://doi.org/10.1016/j.ecoenv.2019.05.065>.
- Zhang, J., Jiang, W., Ning, Z., Wei, C., 2023. Determination of 4 dissolved metals in seawater by direct dilution-inductively coupled plasma mass spectrometry method in press. *Mar. Environ. Sci.* 42 (3).
- Zhang, R., Han, M., Yu, K., Kang, Y., Wang, Y., Huang, X., et al., 2021. Distribution, fate and sources of polycyclic aromatic hydrocarbons (PAHs) in atmosphere and surface water of multiple coral reef regions from the South China Sea: a case study in spring-summer. *J. Hazard Mater.* 412 <https://doi.org/10.1016/j.jhazmat.2021.125214>.
- Zhu, L., Yang, D., Zhang, Z., 2013. Research in large international petroleum companies. South Korea. In: Paper Presented at the 3rd International Conference on Social Sciences and Society (ICSSS), pp. 92–98, 32.